CHAPTER FOUR

4.0 DINDING SCHIST : PHYSICAL AND MECHANICAL PROPERTIES

4.1 Introduction

Several non-destructive and relatively cheap techniques are available for determining the physical and mechanical properties of rocks. Several of these techniques were carried out on block samples of rocks from the study area. Physical properties that were determined include the density, unit weight and apparent porosity; these determinations carried out in accordance with the saturation and buoyancy technique of ISRM (1979). To determine the mechanical properties, several tilt tests were carried out on rock specimens to determine the basic angle of internal friction while hammer rebound values were obtained using a Schmidt hammer model N. With correlation of the different strength properties, it was possible to estimate the shear strength of the rocks in the study area.

Comparison of the physical properties of the rocks obtained in this work with those obtained by Raj (2004) from meta-rhyolitic tuff from the Dinding schist in the Taman Melawati area show fairly narrow differences in the range of values.

4.2 Physical properties of the Dinding schist

In order to determine the physical properties of the Dinding schist, several fresh (unweathered) and slightly weathered rock blocks were collected at various slope cuts in the Taman Ukay Perdana area and sawn into smaller tetrahedral blocks of some 60 cm^3 to 200 cm^3 in volume (Fig. 4.1, Fig. 4.2 and Fig. 4.3). The visible textural and structural features of the individual tetrahedral blocks were then described before their unit weights and apparent porosities were determined, employing the saturation and buoyancy technique of ISRM (1979) (see Appendix 3). Fig. 4.4 show set up of the measurement of saturated weight in air (Wa) whereby the block sample is suspended from the Denver weighing apparatus with a copper wire. Fig. 4.5 show set up of the measurement of saturated weight in water (Ww). The block sample is completely immersed in water while suspended from the Denver weighing apparatus with a copper wire.

Results of the dry density, saturated density, dry unit weight, saturated unit weight, and the apparent porosity of fresh (unweathered) and slightly weathered samples are presented in appendices 4 and 5 respectively.

As shown in Table 4.1, the average dry and saturated unit weights of the weathered samples yielded values of 23.99 kN/m^3 and 24.78k kN/m^3 respectively whereas the average dry and saturated unit weights for the unweathered samples yielded 25.82 kN/m^3 and 26.08 kN/m^3 respectively. Average density values for the weathered samples yielded 2447 kg/m^3 and 2529 kg/m^3 for dry and saturated density respectively. The unweathered samples have average density values of 2636 kg/m^3 for dry and 2661 kg/m^3 for saturated density. Mean apparent porosity is considerably high at 8.2% for weathered samples and low at 2.5% for unweathered samples. In view of the low density and high apparent porosity values of the weathered samples, they are expected to have low strength and high permeability (Zhao and Tohid, 2008). As would be expected, the unweathered samples with lower apparent porosity and higher density values will have comparatively higher strength. The values of the physical properties of unweathered samples during this project were almost of same range as the work done by Bhasin et al (1995).

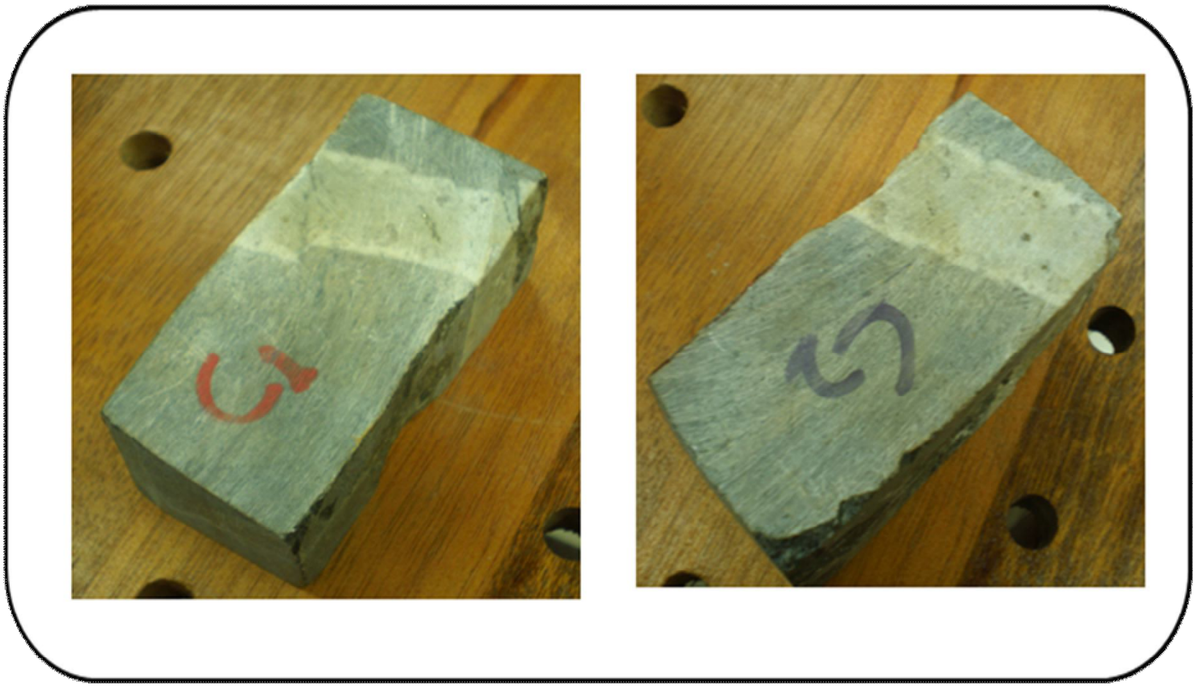

Fig. 4.1: Diamond sawn and highly polished surfaces of block samples.

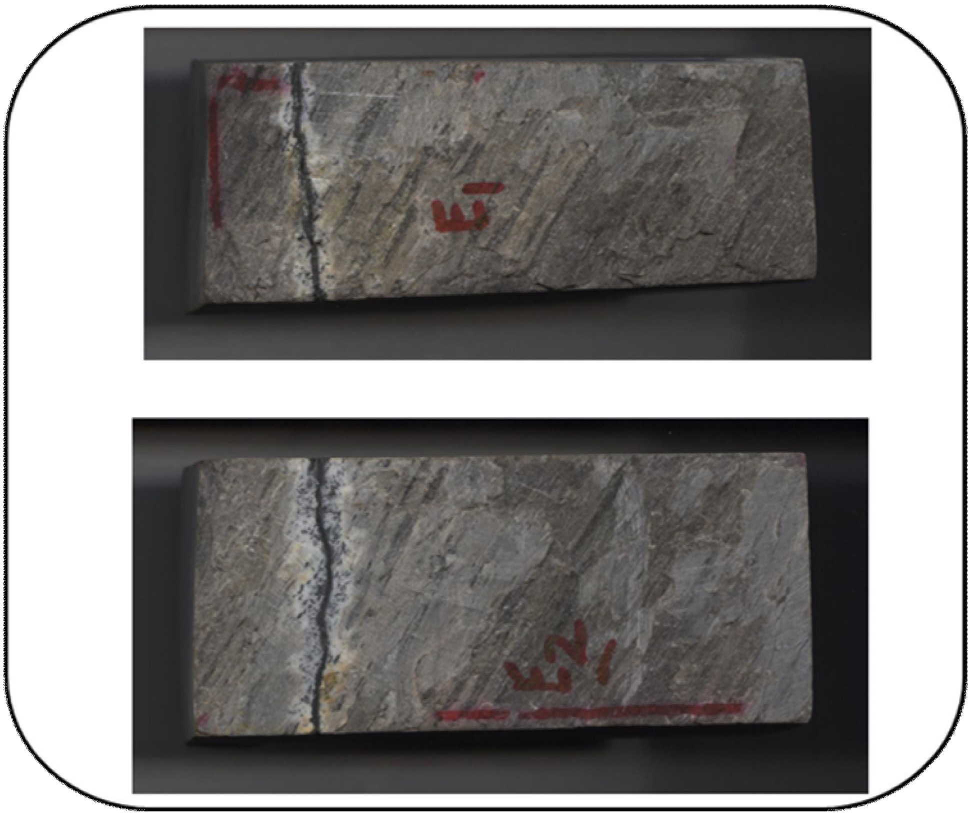

Fig. 4.2: Diamond sawn, but unpolished surfaces of block samples.

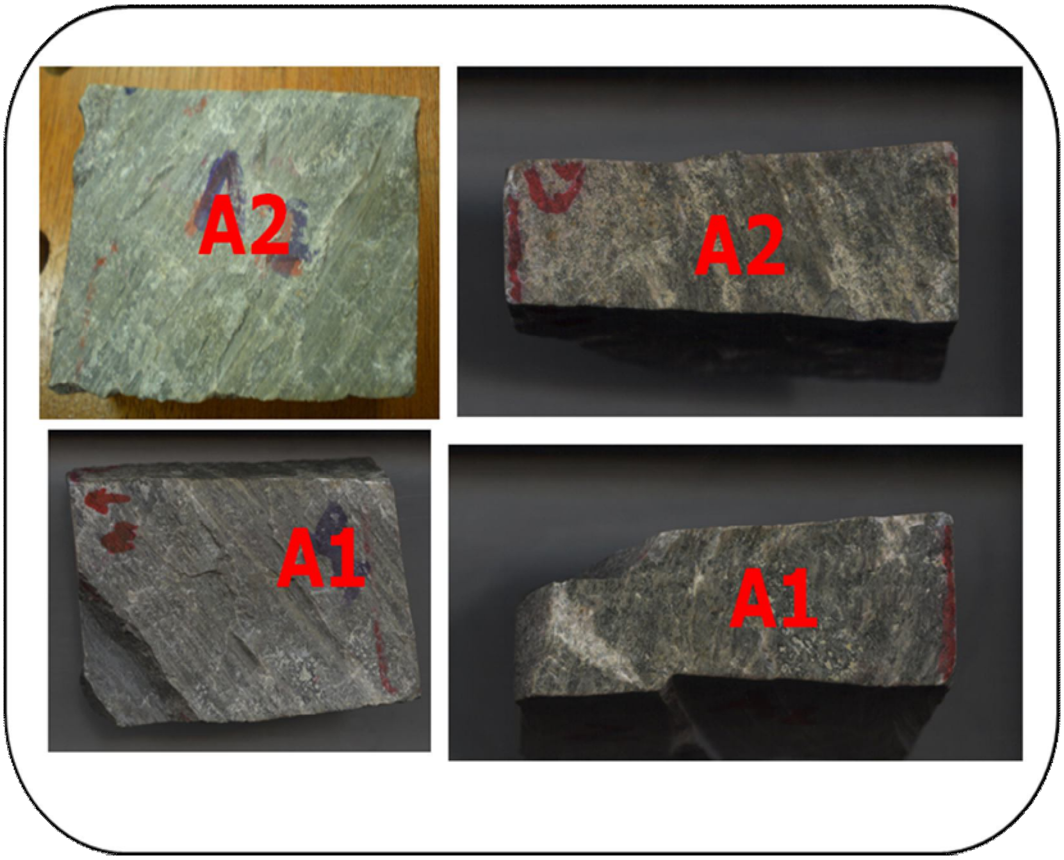

Fig. 4.3: Original discontinuity surfaces of unweathered rock blocks.

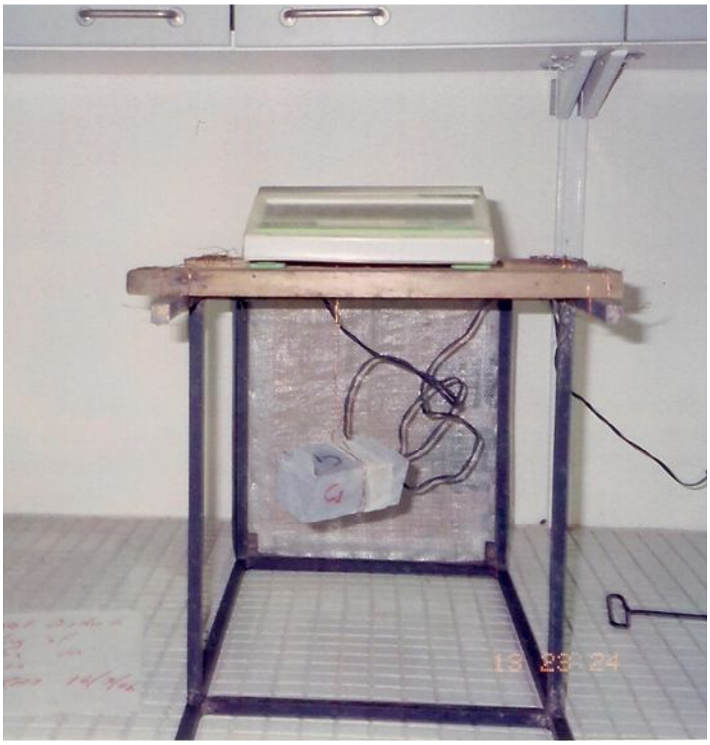

Fig 4.4: Set up of the measurement of Saturated Weight in air (Wa).

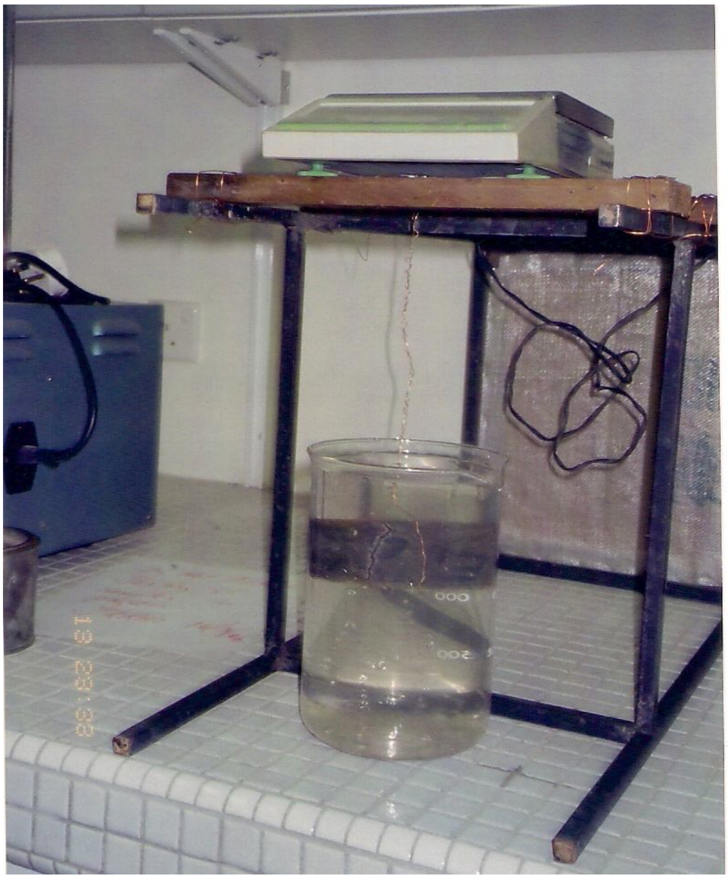

Fig 4.5: Set up of the measurement of Saturated Weight in water (Ww).

	Unweathered	Slightly Weathered
1. Porosity (%)	2.5	8.2
2. Dry unit weight (kN/m^3)	25.82	23.99
3. Saturated Unit Weight (kN/m^3)	26.08	24.78
4. Dry Density (kg/m^3)	2,636.1	2,447.3
5. Saturated Density (kg/m^3)	2660.76	2,528.97

Table 4.1: Physical properties of the Dinding schist.

4.3 Basic Friction Angle

4.3.1 Introduction

All rock masses contain discontinuity planes such as bedding, foliation, cleavage, joint and fault planes and shear zones. These discontinuities or separation planes mainly develop as a result of imposed tectonic stresses and are of variable orientations, extents and spacing. At shallow depths below the earth's surface, where overburden stresses are usually low, failure of intact rock material is minimal and the behavior of rock masses is controlled by sliding along discontinuity planes (Hoek, 2007 in Nkpadobi and Raj, 2008). The shear strength along discontinuity planes is thus of great importance in evaluating the behavior of rock masses at shallow depths.

In view of the high cost of carrying out the large scale testing of discontinuity planes both in the field and in the laboratory, and coupled with difficulties encountered in their interpretations, shear strength determinations nowadays are carried out by measuring the basic friction angle (Φ_b) which is easily measured by testing sawn or ground rock surfaces. As natural discontinuity surfaces are never as smooth as the laboratory tested sawn or ground rock surfaces, however, a correction factor needs to be applied to the basic friction angle in order to estimate the residual friction angle (Φ_r) to be employed in stability analyses. This correction factor for the roughness component is best obtained by visual estimates in the field with several practical techniques described by Hoek (2007).

4.3.2 Tilt tests

Fresh (unweathered) and slightly weathered rock block samples were collected at various cut slopes in the study area, and were sawn into smaller tetrahedral blocks of some 60 cm^3 to 200 cm^3 in volume (Figs. 4.1, Fig. 4.2, and Fig. 4.3). The surfaces of some of the blocks were then lightly, or highly, polished for some 10, and 20 minutes, respectively using a lathe with embedded diamond dust. These blocks were then air dried for 24 hours before tilt tests were carried out. The apparatus for the tilt tests consists of lower holding and upper holding plates with extra plates for loading and tilting (Fig. 4.6) . Upper block (C1) under known load, slides over lower block (C2) when wedge at foot of sample holder is shifted. The method of determination is found in appendix 6.

Results of the tilt tests involving diamond sawn surfaces (cut parallel to foliation) of fresh (unweathered) and slightly weathered samples are given in Appendices 7, 8, 9, 10, 11, 12, ad 13. The basic friction angles (Φb) obtained when the normal and shear stresses acting on the sliding plane are plotted in terms of the Mohr-Coulomb yield criterion (Appendices 14, 15, 16, 17, 18, 19, and 20).

Considering the variations of the physical properties of the Dinding schist and their corresponding basic friction angle (Table 4.2), it is observed that the fresh (unweathered) sample with original discontinuity surfaces has basic friction angle of 26° and a cohesion value of 1.8767 kN/m^2 (appendix 14). This value of cohesion was as a result of interlocking of the discontinuity surfaces thereby causing the breakage of the asperities on the surfaces. Hence the shear stress (τ) required to cause sliding increases with increasing normal stress (σ) (Hoek and Bray 1977).

Apart from samples A1 and A2, the results of the physical properties of samples of the Dinding schists are generally characterized by zero value of cohesion and moderate to high values of basic friction angle.

Fig. 4.6: Set-up of tilt test

Rock Type Surfaces	Dry Density (kg/m^3)	Average Dry Unit Weight (kN/m^3)	Basic Friction Angle Φb (in degrees °)
Naturally exposed unweathered dinding schist. A1 & A2.	2628	25.75	26
Granite vein C1 & C2	2665	26.12	24
Cut but slightly polished and unweathered dinding schist. D1 & D2.	2592	25.33	26
Metasomatised non polished rock surface. E1 & E2.	2660	26.08	30
Slightly weathered dinding schist. B1, B2, and B3.	2447	23.99	28

Table 4.2 : Physical properties of the Dinding schist and corresponding basic friction angles.

4.4 Residual Friction Angle

4.4.1 Correction Factor

Barton and Choubey (1977) found that the residual friction angle (Φ_r) of a joint (the theoretical minimum, with all roughness worn away) is a function of the relative strengths of the joint wall material, and the stronger unweathered material in the interior of each block. As earlier stated, there is a need for a correction factor in estimating this residual friction angle (Φ_r) for slope stability analyses from the basic friction angle (Φ_b) which is easily determined in the laboratory from tilt tests. The correction factor is necessary as natural discontinuity surfaces with their undulations and asperities are never as smooth as the sawn or ground surfaces of rock blocks used in laboratory testing. The correction factor for the roughness component is usually added to the basic friction angle to give the effective friction angle. The roughness component is furthermore, site specific and scale dependent, and is best obtained by visual estimates in the field.

Various authors have demonstrated the influence of the undulations and asperities on a natural discontinuity surface on its shear behavior. Patton (1966) carried out shear tests on saw-tooth specimens to demonstrate this influence. And noted that shear displacements in these specimens occurred as the surfaces move up the inclined faces, thereby causing an increase in volume of the specimens. Patton (1966) represented the shear strength of these saw-tooth specimens by:

$\tau = \sigma n \tan(\varphi b+i)$ ……..equation 1,

whereby i is the angle of the saw-tooth face.

Barton (1973,1976), after studying the behaviour of natural joint rocks, proposed that Patton`s equation be re-written as:

$$\tau = \sigma_n \tan\left[\phi_b + JRC \log_{10}\left(\frac{JCS}{\sigma_n}\right)\right]$$ ……equation 2,

where JRC is Joint roughness coefficient, and

JCS is Joint wall compressive strength.

One of the most useful profile set of joint roughness coefficient was published by Barton and Choubey (1977) and is reproduced in Fig. 4.7. This joint roughness coefficient is a number that can be estimated by visually comparing the appearance of a discontinuity surface with the closest match in the profile. Whereas the joint wall compressive strength can be estimated with the use of the Schmidt rebound hammer (Fig. 4.8) as proposed by Deere and Miller (1966).

The limitation of Patton`s approach is that it does not reflect the reality that changes in shear strength with increasing normal stress are gradual rather than abrupt. Hence Patton`s equation is valid at low normal stress where shear displacement is due to sliding along the inclined surfaces. This is because at normal stresses, the strength of the intact material will be exceeded and the teeth will tend to break off, resulting in a shear strength behaviour which is more closely related to the intact material strength than to the frictional characteristics of the surfaces.

Barton`s equation was revised by Barton and Choubey (1977) to:

$$\tau = \sigma_n \tan\left[\phi_r + JRC \log_{10}\left(\frac{JCS}{\sigma_n}\right)\right]$$ ……..equation 3,

suggesting that residual angle Φr can be estimated from:

$\phi_r = (\phi_b - 20) + 20(r/R)$ ……….equation 4,

Where *r* is Schmidt rebound number on wet and weathered fracture surfaces, and

R is Schmidt rebound number on dry and unweathered sawn surfaces.

Considering this empirical relationship of Barton and Choubey (1977), the estimation of the shear strength of joint rocks is extensively dependent on residual frictional angle (Φ_r), joint roughness coefficient (JRC), and joint wall compressive strength (JCS).

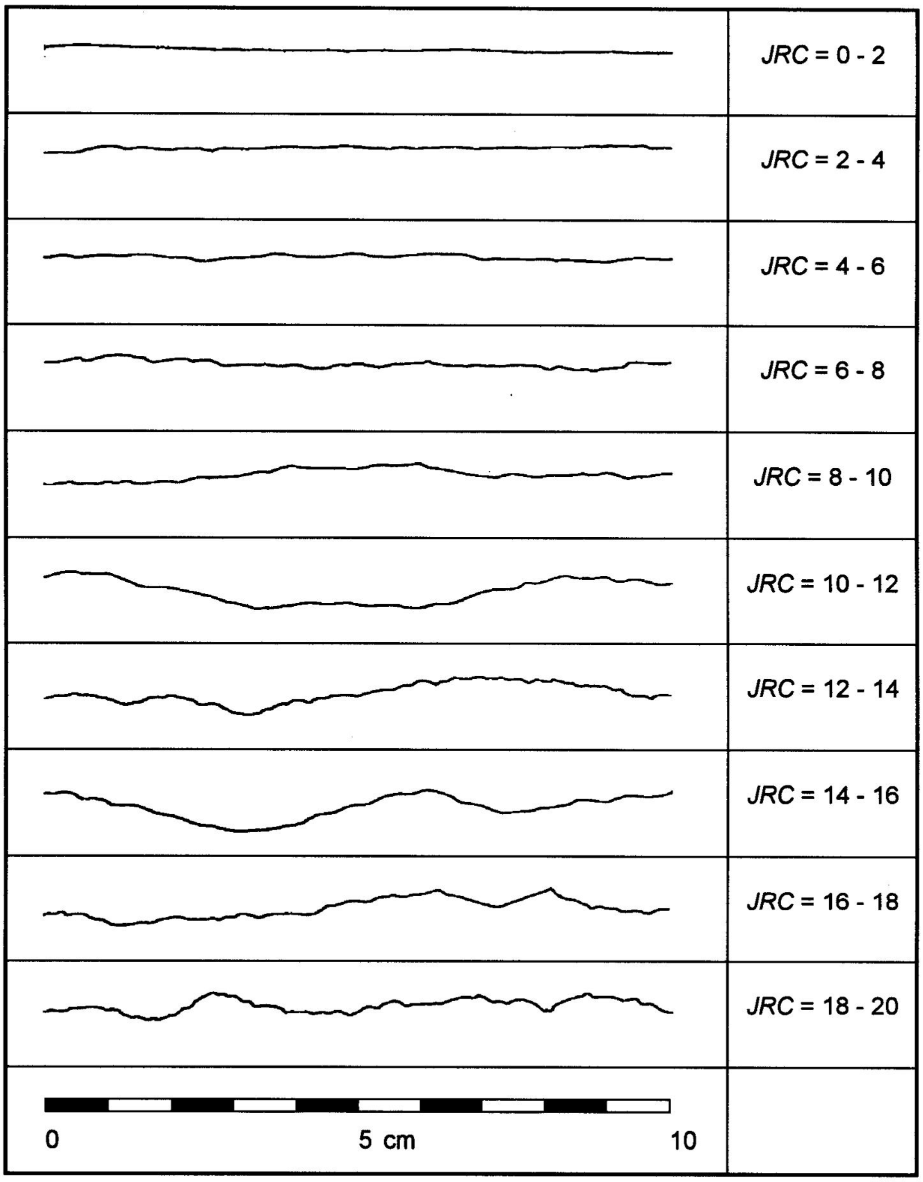

Fig. 4.7: Roughness profile and associated JRC values. (after Barton and Choubey, 1977).

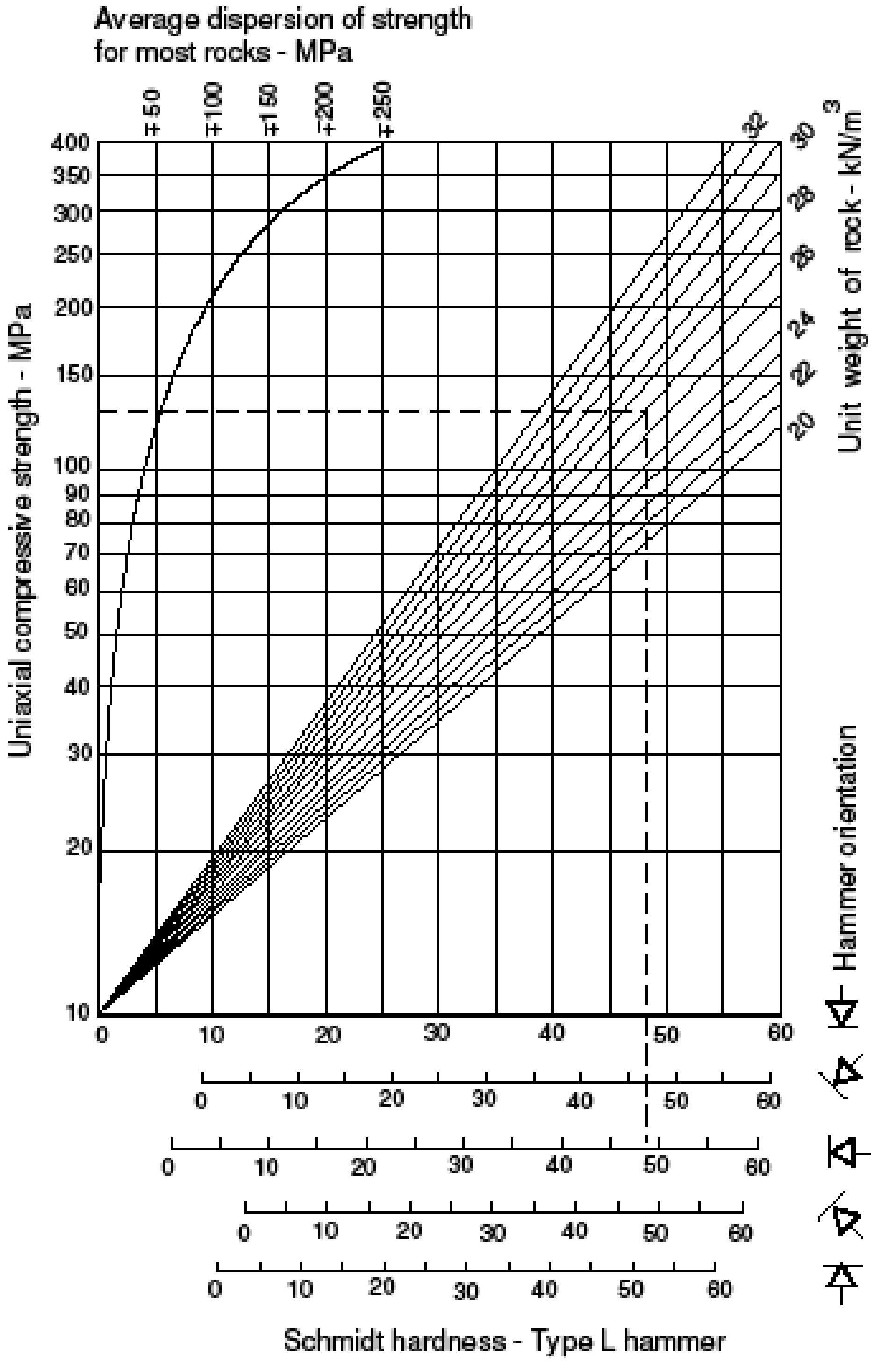

Fig. 4.8. Estimate of joint wall compressive strength from Schmidt hardness (Deere and Miller, 1966).

4.4.2 Schmidt hammer

4.4.2.1 Introduction

The Schmidt hammer was developed for the non-destructive testing of concrete hardness, but has since also been used in testing rock materials. The Schmidt hammer can be used both in the field and in the laboratory, though the size of the tested concrete or rock sample has to be large enough to allow the effect of the non-destructive impact of the hammer. The Schmidt hammer consists of a spring-loaded mass that is released against a plunger when the hammer is pressed onto a hard surface. The plunger impacts the surface and the mass recoils; the rebound value of the mass is measured either by a sliding pointer or electronically, depending on the model of the Schmidt hammer used. The Schmidt hammer rebound numbers; r and R are integral factors for estimation of residual friction angle for slope stability analyses.

4.4.2.2 Method of study

A Schmidt hammer model N was used to investigate the rebound values of in-situ bedrocks in the Taman Ukay Perdana area (Fig 4.9). Field measurements on both dry and wet outcrops were carried out on four types of surfaces; naturally exposed unweathered rock surfaces, cut but unpolished rock surfaces, slightly weathered rock surfaces, and rock surfaces polished manually with the grinding stone provided by the hammer manufacturer. Schmidt hammer tests were also carried out on granite veins and metasomatised rocks in the area.

These Schmidt hammer measurements were carried out at the various dry outcrops where the samples for determination of physical properties had been collected. The measurements on wet outcrops in same locations were carried out after short intense rainfall. Prior to each test, the impact area was inspected for macroscopic defects to avoid testing near fractures or material in-homogeneities. At each location, more than 20 rebound values were measured with a minimal separation of the plunger diameter between impact locations. This separation ensures that the impacts hit undamaged rocks. The mean rebound value at each location was then obtained (Table 4.3). The Schmidt hammer rebound R range of 40-62 corresponds with the dry density range of 2447 kg/m^3 - 2665 kg/m^3. Fig. 4.10 shows empirical relations between hammer rebound values and the measured dry density obtained from standard method of ISRM, (1979).

The correlation factor in the graphic equation is:-

$y=459.6Ln(x)+805.4$

$R^2=0.761$,

and can be used to estimate the relevant mechanical properties in the field and laboratory. Thus the joint wall compressive strength (uniaxial compressive strength) can be estimated with the use of the Schmidt hammer data as shown in Fig 4.11 and the joint roughness coefficient can be estimated by visually comparing the appearance of a discontinuity surface with the closest match in the profile after Barton and Choubey, 1977.

4.4.3 Estimation of Residual Friction Angle

The value of basic friction angle is always considered to be less than or equal to the value of residual friction angle (Giani 1992; US Patent 1994; Barton 2006). Substituting the Schmidt hammer rebound values on wet and dry in-situ bedrocks and the basic friction angles Φb for all rock surfaces in equation 4, the residual friction angle can thus be estimated (Table 4.11). The values of residual friction angle for all rock surfaces are quite moderate for both weathered and unweathered schist. As shown in fig. 4.11 and Table 4.3, apart from the granite vein with high strength value, further estimation of joint wall compressive strength (uniaxial compressive strength) with the use of the Schmidt hammer rebound value R show medium strength values of uniaxial compressive strength which indicate that the rock mass is of relatively moderate shear strength.

Fig. 4.9. The writer using the Schmidt hammer model N on in-situ rocks in Taman Ukay Perdana.

Rock Type Surfaces	Schmidt Hammer Mean Rebound R (on dry in-situ bedrock)	Schmidt Hammer Mean Rebound r (on wet in-situ bedrock)	Dry Density (kg/m³)	Average Dry Unit Weight (kN/m³)	Basic Friction Angle *Φb* (in degrees°)	Residual Friction Angle *Φr* (in degrees°)	Uniaxial compressive strength (MPa)
Naturally exposed unweathered dinding schist A1 & A2	51	25	2628	25.75	26	16	140
Granite vein C1 & C2	62	50	2665	26.12	24	20	240
Cut but unpolished and unweathered dinding schist D1 &D2	44	24	2592	25.33	26	17	98
Metasomatised polished rock surface. E1 & E2	53	33	2660	26.08	30	24	162.5
Slightly weathered dinding schist B1, B2, & B3	40	13	2447	23.99	28	15	72

Table 4.3. Schmidt hammer data and mechanical properties of investigated rocks.

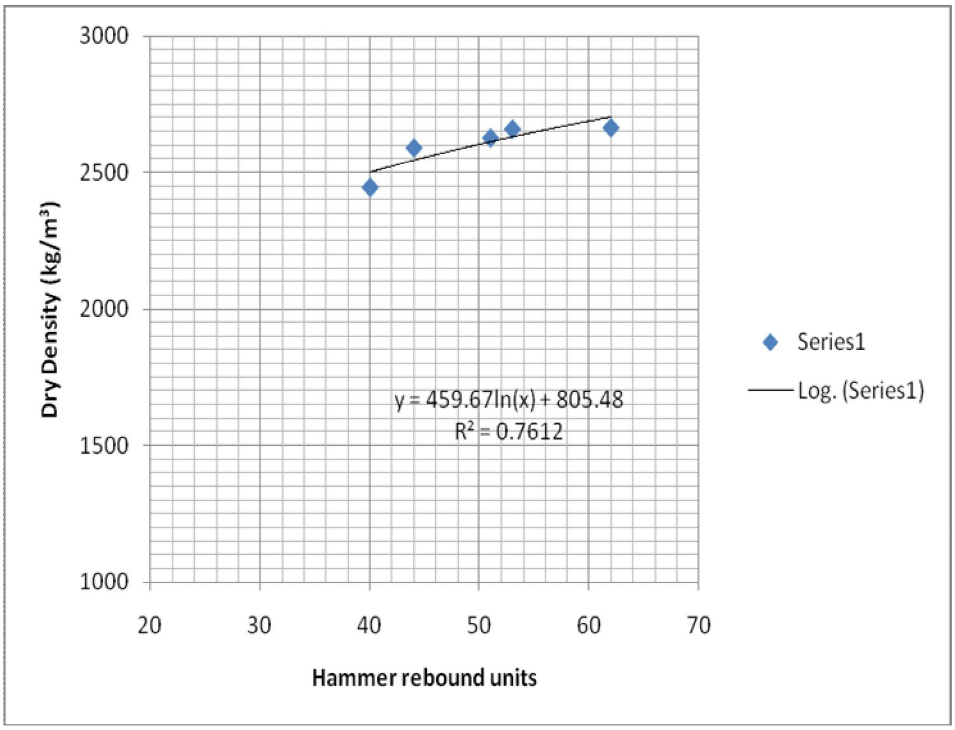

Fig 4.10. Empirical relations between hammer rebound values and the measured dry density.

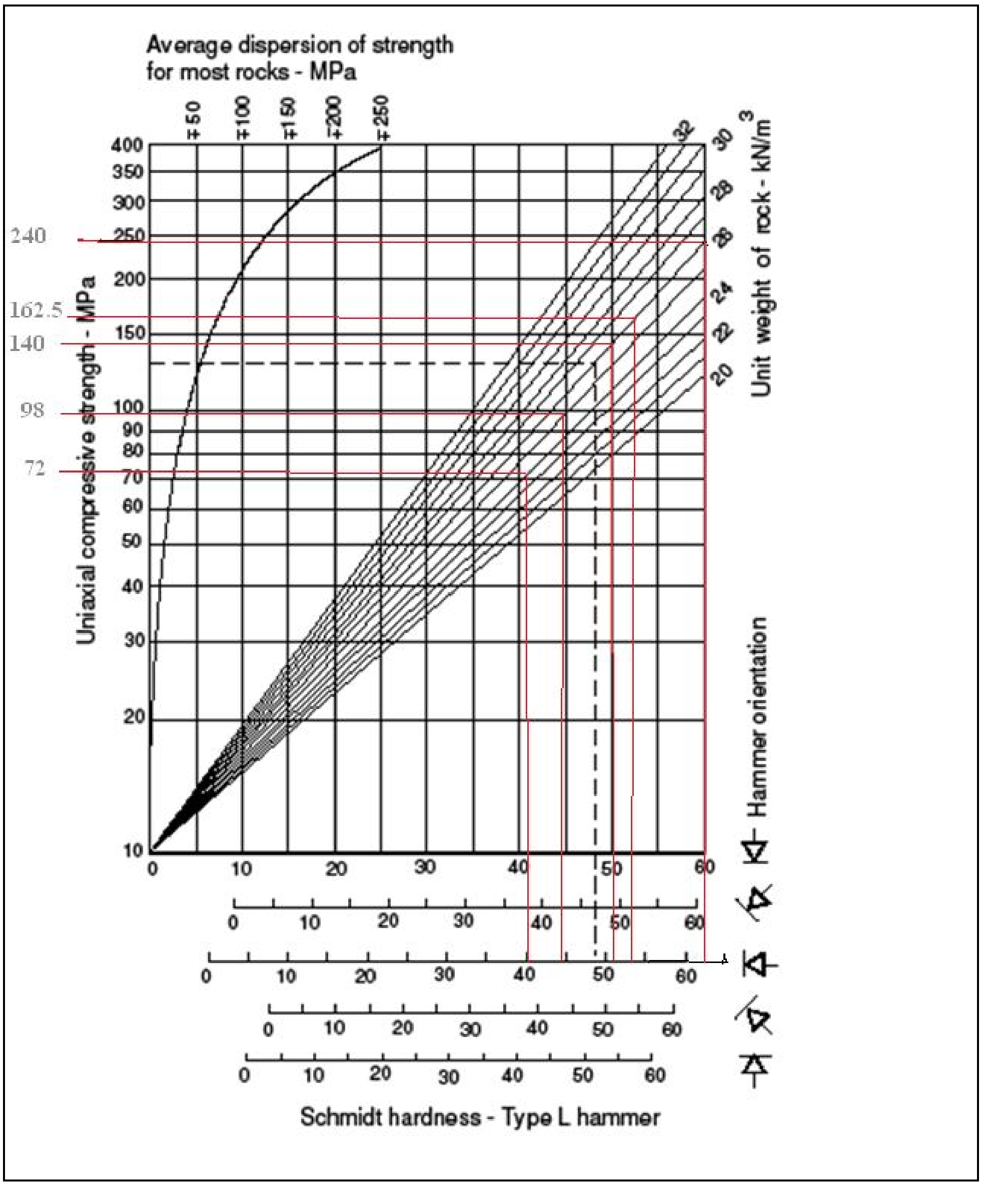

Fig. 4.11. Estimation of joint wall compressive strength (uniaxial compressive strength) with the use of the Schmidt hammer data

4.5 Weathering

4.5.1 Introduction

Weathering and future weathering after construction of a slope is considered by Marinos et al (1997) as the main cause for failure of a slope during its engineering life-time. The influence of weathering is related to the rock mass weathering as described by BSI 5930 (1981). The weathering processes often are slow (hundreds to thousands of years). The amount of time that rocks and minerals have been exposed at the earth's surface will influence the degree to which they have weathered. Weathered material may be removed leaving a porous framework of individual grains, or new material may be precipitated in the pores, at grain boundaries or along fractures. In this research, significant understanding on the impact of weathering and weathering processes on the Dinding schist has been gained through field and laboratory investigations of the physical and mechanical properties of the rocks as well as published literature. Considerable efforts have been made to identify the effects of weathering on the stability of the cut slopes in the study area. There are distinct variations in the values of the physical and mechanical properties of the fresh (unweathered) and slightly weathered samples used in this research. Various authors (including Marinos et al 1997; and Bell, 2000) have studied the effect of weathering on quartz-mica schist in different locations in relation to slope failures. But published data on the effect of weathering in relation to slope failures in the study area is limited (apart from Raj, 1983,) who studied the failures of slopes cut in the residual soils over the Dinding schist. With the study of physical and mechanical properties of rock samples, Nkpadobi and Raj (2008) provided data on the basic friction angle of foliation planes in the meta-rhyolitic tuff of the Dinding schist.

Weathering is not only dependent on the mineral composition but also on the porosity of the rock (Robinson and Williams, 1994). The rate of weathering is influenced by temperature, rate of water percolation and oxidation status of the weathering zone. The resistance to weathering of rock however, depends on types of mineral present, surface area of rock exposed and porosity of rocks. Therefore a considerable degree of resistance to weathering is identified in the rocks of the Dinding schist because quartz which is the major mineral consists entirely of linked silicon tetrahedral.

Weathering processes identified in the study area are mechanical (physical) and chemical weathering. There is a possibility of a biological weathering in the area but the confirmation was hindered by inaccessibility to the uppermost region of the slope cuts where organisms assist in breaking down rock into sediment or soil.

Mechanical weathering disintegrates the rock into smaller and smaller fragments with little or no change in chemical composition. Several processes that can result into this disintegration as outlined by Raj (2000) include:

i. Pressure release due to erosional unloading, leading to development of sheeting joints over large intrusive igneous rock bodies, or the opening-up of tight or closed discontinuity planes such as bedding, joint, fault, cleavage, foliation etc.

ii. Growth of foreign crystals in rock as in the frost wedging when water trickles down into fractures and pores of rock, then freezes (its volume increasing up to 9%), or during the formation of hydrates (as gypsum form anhydrates with up to 140% volume increase).

iii. Thermal expansion and contraction due to alternate heating and cooling as very hot days and cool nights or forest fires and thunder storms (not confirmed experimentally).

iv. Biological agents, as wedging action of roots and burrowing activities of earthworms and other organisms.

Chemical weathering however, transforms the original material into a substance with a different composition and different physical characteristics. The new substance is typically much softer and more susceptible to agents of erosion than the original material. The rate of chemical weathering is greatly accelerated by the presence of warm temperatures and moisture. Also some minerals are more vulnerable to chemical weathering than others. For example, feldspar is more reactive than quartz. Several reactions involved in chemical weathering include:

i. Dissolution (or solution)- where several common minerals dissolve in water with change or no change in chemical composition.

ii. Oxidation- where oxygen combines with iron-bearing silicate minerals causing "rusting".

iii. Hydrolysis- silicate minerals weather by hydrolysis to form clay.

4.5.2 Weathering of the Dinding schist

The Dinding schist otherwise called quartz-mica schist is created as a result of directed pressure and heat causing major re-crystallization of the original minerals, thus giving rise to new minerals especially micas and having a foliated appearance. The gradual reduction in hardness from the interior to the slope surface was recognized within slopes. The hardness change as confirmed with Schmidt hammer measurements where almost concordant with changes in other weathering indices such as rock colour, presence of clay minerals, and apparent grain size. Fig. 3.3 clearly shows that weathering of the quartz-mica schist rock materials involves its staining, discoloration, and gradual degradation. Although the extent of alteration of original mineral grains and the extent of staining characterize the distinct stages of weathering of the Dinding schist, some of their physical properties considered on the scale of hand specimen also gave descriptive and index rock properties. The bedrock consists essentially of fine grained quartz crystals that form thin bands in parallel alignment with variable amounts of biotite, muscovite, chlorite, and sericite flakes. The clay minerals largely resulting from the alteration of micas, are also frequently found and are mainly responsible for the dark colour of the bedrock (Raj 1983).

In addition to the exposed unweathered bedrock at the weathering profile, four morphological zones and their estimated corresponding thicknesses were distinguished; unweathered bedrock, slightly weathered, moderately weathered, and highly weathered (Fig. 4.12).

The unweathered bedrock show no visible sign of rock material weathering, though there were some discoloration on major discontinuity surfaces. In the slightly weathered, there is reddish brown discoloration along discontinuity planes. The mass structure and material texture are completely preserved. However, the material is generally weaker but fragment corners cannot be chipped by hand. The moderately weathered rocks show partial discoloration of reddish yellow, but the mass structure and material texture are completely preserved. Discontinuity planes in the moderately weathered rocks are commonly filled by iron-rich material, and the material fragment or block corner can be chipped by hand. Fig. 4.13 shows the boundary between slightly weathered and moderately weathered zones.

For the highly weathered, the rock material is in the transitional stage to form soil. In fact the material condition is either soil or rock, but the mass structure is partially present. The material is completely discoloured to yellowish red, but the fabric is completely preserved. In most cases, the relics of moderately weathered units are found in-between the highly weathered zones as shown in Fig. 4.14.

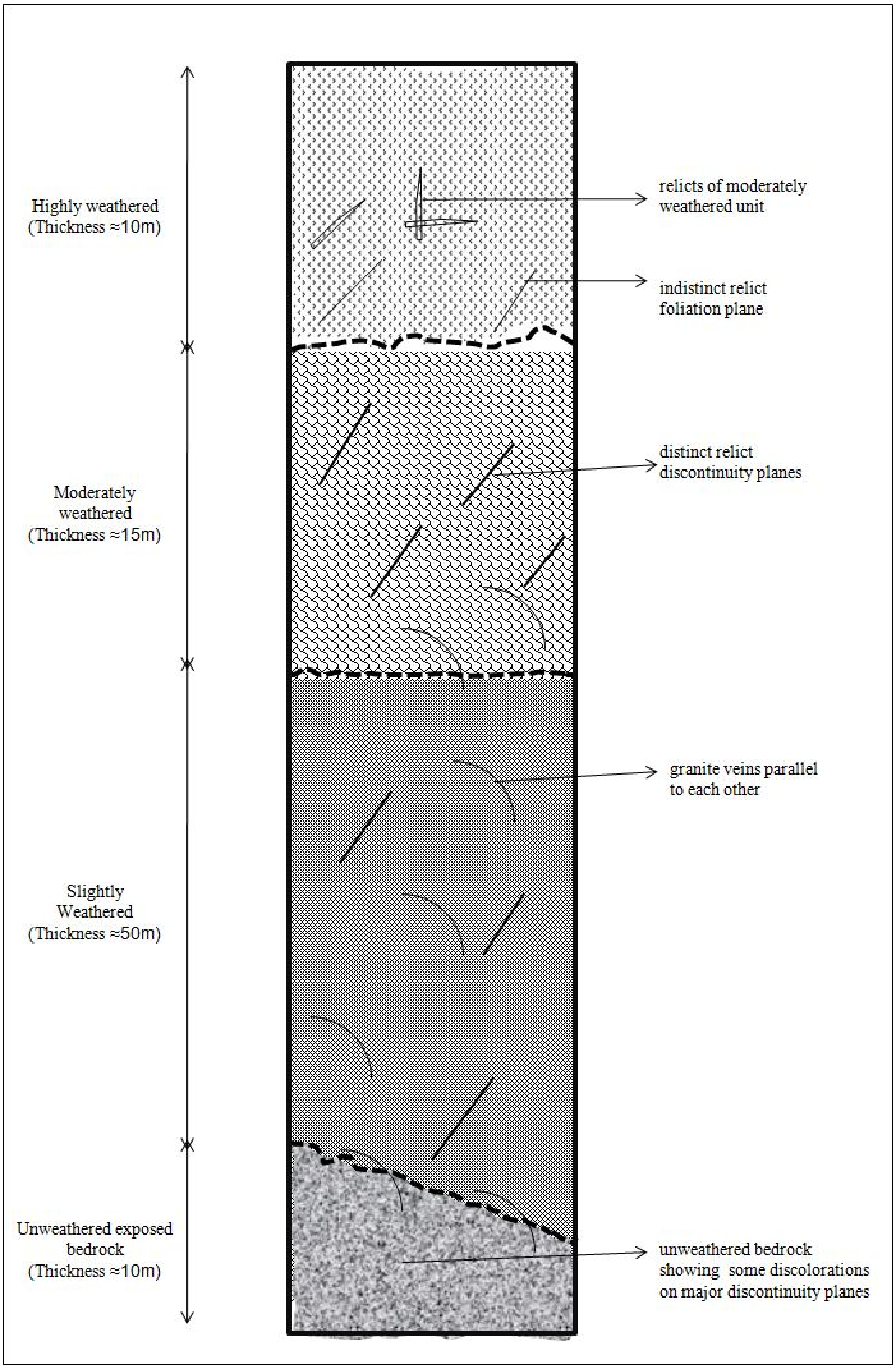

Fig. 4.12: Schematic sketch showing the different morphological zones of the weathering profile.

Fig. 4.13: Gradual degradation of exposed bedrock from slightly weathered to moderately weathered unit.

Fig. 4.14: Exposed highly weathered zone with visible relicts of moderately weathered units found in-between.

4.5.3. Summary on weathering

Most engineering works are confined to shallow depths where weathering has a dominant role to play and affects almost all the properties of rocks (Gupta and Seshagiri, 2000). The properties of the rocks change as weathering continues, and the stages of weathering is transitional or gradational in that each stage of weathering gradually develops into another. Hence weathering leads to progressive failure. Chemical weathering observed in the Dinding schist slowly weakens slope material (primarily rock), reducing its shear strength, therefore reducing resisting forces. The weathered zones indicated by the reduction in hardness (which correlates with their strength), staining and discoloration, are frequently subjected to gullying and surface failures. However, failures in the study area were not limited to weathered zones.